

Investigation of Mach Number Independence Principle for a Two-Dimensional Wedge

¹Shivashree S

¹Jain (Deemed-to-be) University, Bangalore, India, E-mail: Shivashrees2017@gmail.com

ABSTRACT: Oswatitsch's independence principle depicts an important role in aerothermodynamics. For instance, force coefficients for a given body shape which are obtained experimentally at a large Mach number $M_{\infty 1}$ will be valid for all larger Mach numbers i.e., $M_{\infty 2} > M_{\infty 1}$, provided the flow is inviscid and perfect gas. However, at a high temperature above the wall, the Mach number begins to lose its validity. This paper analyzes a slender 2D wedge numerically and theoretically within a range of $2 < M_{\infty} < 20$ for certain aerodynamic properties: such as pressure coefficient, wave-drag coefficients, and shock wave angle which have been important for the design of high-speed vehicles. Computational studies were performed to inspect the wedge for Mach number independence through FLUENT and the applicability of the principle is examined by considering an adiabatic wall boundary condition. Numerical results of C_p , C_D , and shock wave angle show fairly good agreement with the theoretical results. For the slender wedge taken into account here at high Mach numbers, the Mach angle could be of the same magnitude as the maximum deflection angle, which the flow undergoes at the body surface.

Keywords: Independence principle, Inviscid, 2D wedge, Aerodynamic properties, Adiabatic, High mach numbers

INTRODUCTION

In the vicinity of the Mach number independence principle, Oswatitsch involved the basic hypersonic limiting process $M_{\infty} \rightarrow \infty$. From his analysis, he deduced that for a very high Mach number, the drag coefficient, pressure coefficient, and shock wave patterns on a body are independent of the value of M_{∞} . These properties can be measured at a lower Mach number for the ground test facilities in the test section. Concurrently, this result was proved by Sir Isaac Newton for his model of rarefied gas. However, the principle has been derived for calorically perfect gas and inviscid flow only. Mathematically phrased, the Mach number independence principle states that if density and velocity are fixed, the solution within a fixed finite domain approaches a limiting solution uniformly in the limit M_{∞} .

For atmospheric controlled entry (re-entry) type flight vehicles such as suborbital, orbital, and super-orbital vehicles, various advanced technologies have been developed to perform experiments on the flight at extreme velocities. At present Lens-X is the only wind tunnel with a top speed of Mach 30. However, atmospheric entry interface velocities are on the order of 12Km/s, i.e., in the range of Mach 35. Given this, Oswatitsch's independence principle plays a considerable role in analyzing the aerodynamic properties.

Despite these advantages, the principle indicates that independence exists for constant unit Reynolds number. It is important to note that, as in hypersonic continuum flow, the Mach number independence principle is operative at much lower speed ratios for blunt bodies than for slender bodies.

LITERATURE SURVEY

Several articles are presented in the literature concerning the Mach number independence principle for blunt bodies but a study on a slender body is scant. Scaling the data, Claus Weiland et al. [15] studied that the Sanger flow field is more friction-dominated than few fields of the re-entry vehicles. Volkmar Lorenz, Christian Mundt, et al. [16] studied that lower ratios of specific heats require a lower Mach number to achieve Mach number independence. Sphere drag forces at subsonic, transonic, and supersonic velocities were studied by Charters and Thomas. et al. [2]. The Mach Number range was 0.29 to 3.96 and the corresponding Reynolds Numbers varied from 9.3×10^4 to 1.3×10^6 . For Reynolds Numbers of the order of magnitude 10^5 . They found no Reynolds Number effect at supersonic velocities, and they demonstrated that the drag coefficient could be correlated as a function of Mach Number alone. A. J. HODGES [5] in his work reported that drag coefficients of spheres in the air were determined at Mach numbers ranging from 2.2 to 9.7. The data indicates that at Mach numbers ranging from 4 to 10 the drag coefficient of spheres in the air does not vary significantly. D. Kliche [4] verified numerically that for viscous flow and adiabatic wall, the aerodynamic coefficients show the same behavior as for inviscid flow. Hayes and Probstein [7] stated that the principle also holds for viscous flow and high-temperature real-gas effects. Here, we find that the Mach number independence is defined for blunt bodies where an intense increase in heat flux

could cause shear layer attachment or boundary layer interaction which in turn causes adverse pressure gradient and which also increases the transition Reynolds number relative to that of a sharp-nosed wedge.

THE OBJECTIVE OF THIS STUDY

In this paper for slender bodies considered here, we peruse the numerical and theoretical results, giving insight into how certain properties such as drag coefficient, pressure coefficient, and shock wave patterns behave at high Mach numbers. The inviscid flow past an axisymmetric 2D wedge is analyzed using Oswatitsch's independence principle.

INLET GEOMETRY AND DEFINITIONS

Figure 1 shows the plane view and geometric configuration of the 2D wedge model designed in CATIAV5. The ramp generates oblique shock at speed $M_\infty > 1$. The shocks in turn deflect the freestream flow to a certain angle. The ramp is composed of a width of 1.004m inclining at 4.8 deg.

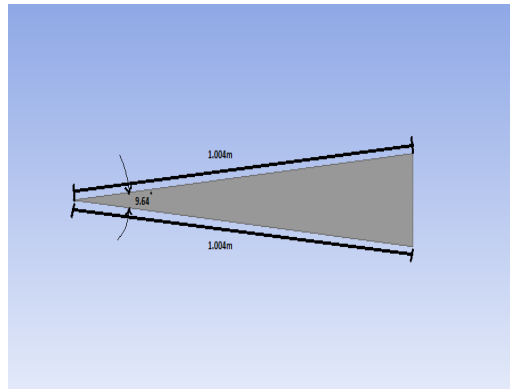


Figure 1-Plane view of the 2D wedge

GOVERNING EQUATIONS

Considering the hypersonic limit $M_\infty \Rightarrow \infty$ results in a set of mach number independent equations. To solve for the hypersonic flow field using the known governing equations and the boundary conditions at the wall, we assume that the location and shape of the shock are known to us and we are intended to solve for the flowfield in the shock layer or the volume between shock and body. This technique is called a shock fitting technique.

Rankine-Hugoniot relations for the oblique shock wave can be defined as,

$$\frac{P_2}{P_1} = \left\{ \frac{[4\gamma M_1^2 \sin^2 \beta - 2(\gamma - 1)][(\gamma - 1)M_1^2 \sin^2 \beta + 2]}{(\gamma + 1)^2 M_1^2 \sin^2 \beta [(\gamma - 1)M_1^2 + 2]} \right\}^{\frac{\gamma}{\gamma - 1}}$$

$$\frac{u_2}{V_1} = 1 - \frac{2(M_1^2 \sin^2 \beta - 1)}{(\gamma + 1)M_1^2}$$

$$\frac{v_2}{V_1} = \frac{2(M_1^2 \sin^2 \beta - 1)}{(\gamma + 1)M_1^2} \cot \beta$$

$$\frac{V_2^2}{V_1^2} = \frac{4(M_1^2 \sin^2 \beta - 1)(\gamma M_1^2 \sin^2 \beta + 1)}{(\gamma + 1)^2 M_1^4 \sin^2 \beta}$$

Below relations define what is called Oswatitsch's independence principle, which is obtained by limiting the Mach number in above relations to infinity.

$$\frac{p_2}{p_1} = \left\{ \frac{4\gamma \sin^2 \beta}{(\gamma+1)^2} \right\}^{\frac{\gamma}{\gamma-1}}$$

$$\frac{u_2}{V_1} \rightarrow \frac{\gamma-1}{\gamma+1} \sin \beta$$

$$\frac{v_2}{V_1} = \cos \beta$$

$$\frac{V_2^2}{V_1^2} = 1 - \frac{4\gamma \sin^2 \beta}{(\gamma+1)^2}$$

Other flow parameters that are used to find the relation between shock angle " β ", and ramp angle " θ ", i.e. the deflection angle in terms of upstream Mach number, and specific heat ratio γ are,

$$\square \quad \tan \theta = 2 \frac{2 \cot \beta (M_1^2 \sin^2 \beta - 1)}{2 + M_1^2 (\gamma + 1 - 2 \sin^2 \beta)}$$

As $M_1 \rightarrow \infty$

$$\beta \rightarrow \frac{\gamma+1}{2} \theta$$

$$\square \quad C_p = \frac{4(M_1^2 \sin^2 \beta - 1)}{(\gamma+1)M_1^2}$$

As $M_1 \rightarrow \infty$,

$$C_p = \frac{4 \sin^2 \beta}{(\gamma+1)}$$

$$\square \quad M_2^2 = \frac{(\gamma+1)^2 M_1^4 \sin^2 \beta - 4(M_1^2 \sin^2 \beta - 1)(\gamma M_1^2 \sin^2 \beta + 1)}{[2\gamma M_1^2 \sin^2 \beta - (\gamma-1)][(\gamma-1)M_1^2 \sin^2 \beta + 2]}$$

As $M_1 \rightarrow \infty$,

$$M_2^2 = \frac{(\gamma+1)^2 - 4\gamma \sin^2 \beta}{2\gamma(\gamma-1)\sin^2 \beta}$$

NUMERICAL DETAILS

The governing equations are numerically solved using a Two-dimensional density-based solver. An inviscid turbulence model is applied to simulate the flow condition over the wedge and the standard wall function is used to model the flow near the region of the wall. These equations are discretized by integrating over a rectangular control volume. The turbulent intensity and turbulent viscosity ratio are set to 0.5% and 5 respectively. The Courant number is set to less than one. The flux term is solved with the Roe-FDS scheme. The spatial discretization was carried out using the Green-Gauss Cell-Based gradient to get better convergence. The 1st-order upwind scheme is used followed by the 2nd order to discretize the equations spatially and to get a stable initial flowfield. A second-order implicit scheme has been used to discretize the time derivatives. The solution is being initialized using hybrid initialization based on the solving of Laplace equations to determine the pressure and velocity parameters. The calculations were run with solution steering on. The solution is assumed to be converged when the divergence in each cell falls well below 10^{-4} .

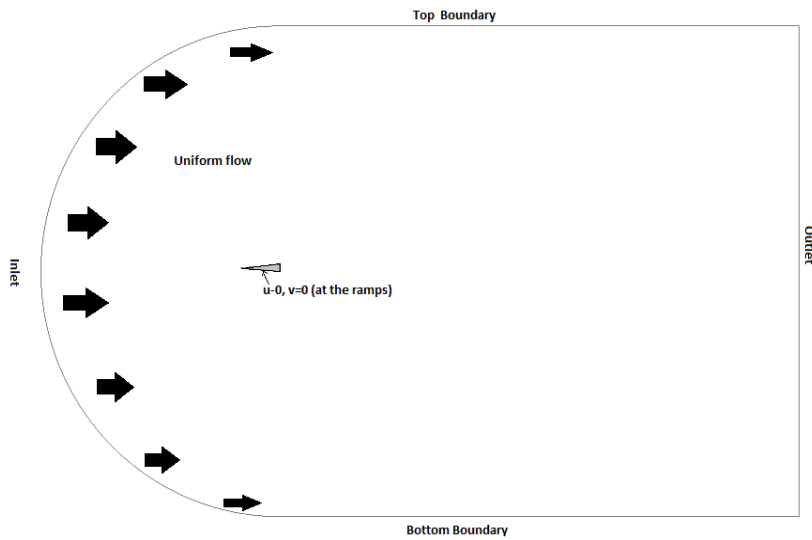


Figure 2-Computational Domain of the Wedge

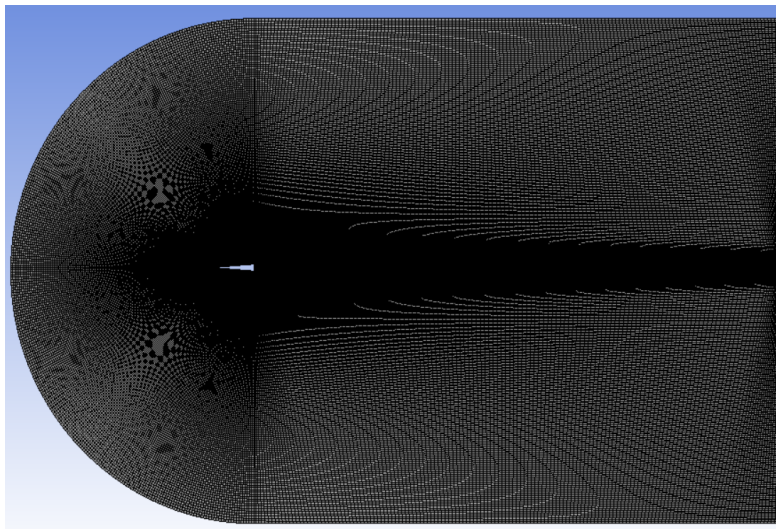


Figure 3-Mesh distribution in the vicinity of the wedge

A. SIZE OF THE COMPUTATIONAL DOMAIN

The fluid domain is far enough away from the model to apply the pressure far-field boundary condition in Fluent. The fluid domain will have a structured mesh with quad elements growing larger as they are farther away from the wedge. For Mach numbers greater than one, the domain size can be small enough as the disturbances cannot work their way upstream. The near-wall y^+ is less than 5 to capture the surface boundary layer accurately. The pressure far-field boundary condition is set on the inflow surface, whereas the pressure outlet is set on the exit surface.

B. GRID INDEPENDENCE TEST

A high Mach number flow case $M_\infty=5$ and $\gamma = 1.4$ was selected to show the grid-independent solution. The drag coefficient C_D was chosen and numerical experiments were performed for various grid sizes. The following three different mesh sizes have been used to check the grid's dependence on the average drag coefficient C_D . The minimum distance of the first grid point from the inlet wall is 0.001. The dependence of mesh size on C_D is presented in Table 1. Looking at Table 1, one can find that Mesh B and C produce grid-independent results with the changes in C_D occurring only at the fifth decimal place. Hence, Mesh B is chosen for further computation as it presents the best flow field with the least computational time.

Table 1

Grid Sensitivity	Grids (m × n)	Average drag coefficient C_D
Grid A (Coarse)	100 × 120	0.10425
Grid B (Medium)	400 × 410	0.105007
Grid C (Fine)	500 × 716	0.105016

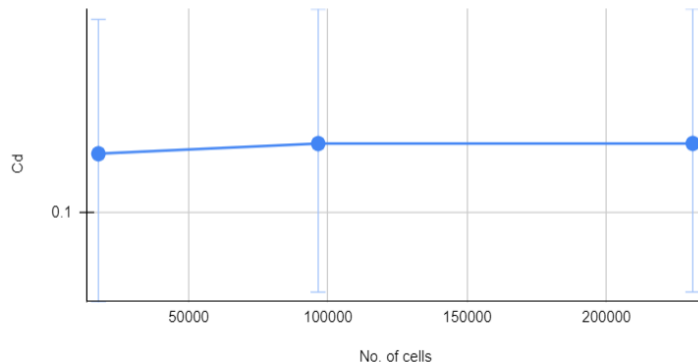


Figure 4-Grid independence study of the wedge

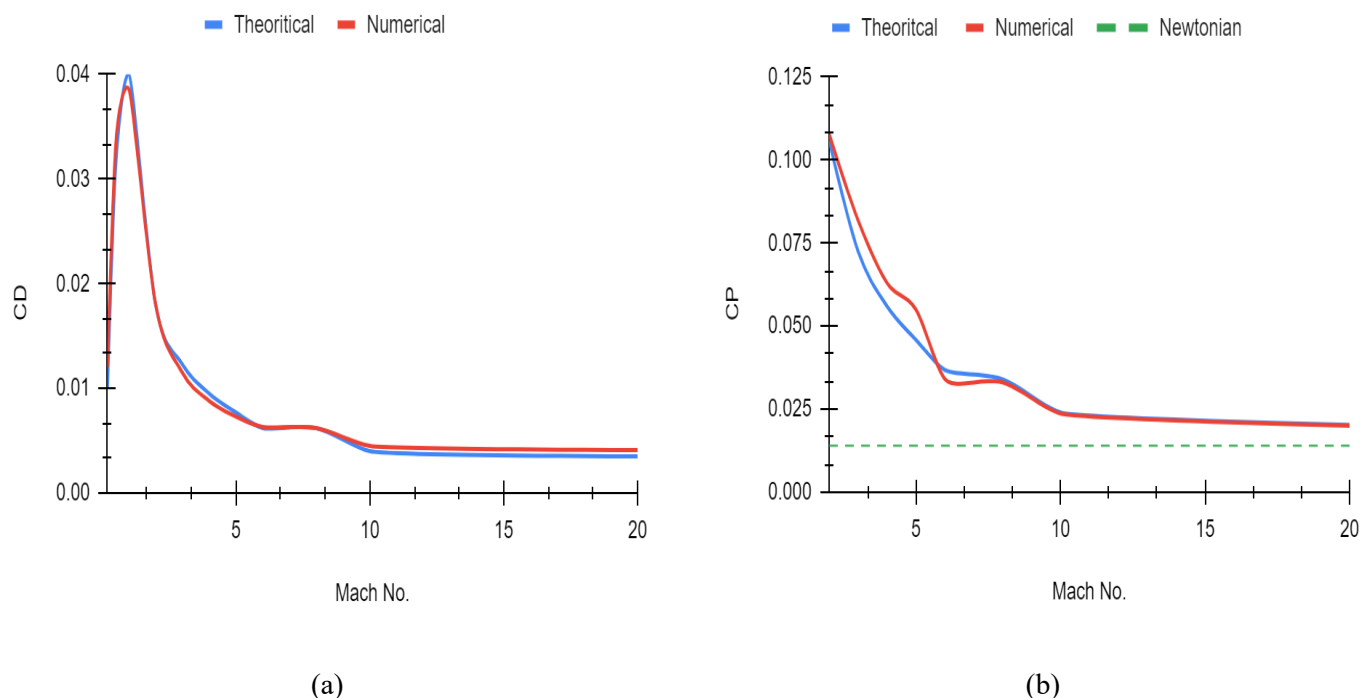


Figure 5- Variation of drag coefficient (a) and pressure coefficient with Mach number

RESULTS AND DISCUSSIONS

Numerical simulations from Mach 1 to Mach 20 are carried out using Fluent with the inviscid flow equations for the above-defined wedge. These results will enable us to evaluate whether aerodynamic coefficients such as pressure coefficients, wave drag coefficients, and shock wave shapes become independent of mach number at pressure and temperature of 2.8KPa and 220K respectively.

1. EVALUATION OF DRAG COEFFICIENT

The drag is essentially a wave drag at hypersonic speeds. The source of wave drag is the pressure distribution exerted over the surface and is a result of shock and expansion wave pattern in the flow over the wedge. For cases other than inviscid flow, the value of friction drag is also neglected due to an increase in Reynolds number with increasing Mach number. But the decrease in C_f is more significant for a turbulent boundary layer than a laminar boundary layer, Ref[3]. Here, as the flow regime changes from incompressible to transonic zone, drag coefficient increases which are associated with the drag divergence theorem. Further, an increase in Mach number leads to a decrease in C_D to 0.0041 till $M_\infty=10$, and Oswatitsch principle is attained as M_∞ becomes large. Fig.5a shows numerical and theoretical wave-drag coefficient as a function of Mach number in calorically perfect air for inviscid flow. Numerical C_D deviates from the theoretical C_D by an average of 11%.

Spheres and cones have relatively lesser drag due to the three-dimensional relieving effect compared to the slender body. The data for spheres from Ref[5] indicates that at Mach Numbers ranging from 4 to 20 the drag coefficient does not vary significantly. Whereas for slender configurations with a pointed nose, like the hypersonic cruise vehicle Sanger Ref[15], this occurs in principle at higher Mach numbers where viscous effects play a major role. It should be noted that the discontinuity increases the drag for a very thin body, but that for thicker bodies, this is not so.

2. EVALUATION OF PRESSURE COEFFICIENT

In aerodynamics, pressure distributions are usually quoted in terms of the pressure coefficient. Approximated linearized theory can be utilized to define C_p , as waves of finite strength are not taken into account. For small perturbations, C_p is directly proportional to the surface inclination of the wall concerning the freestream which only holds for the slender two-dimensional body where " θ " is

relatively small. Fig.5b shows numerical and theoretical pressure coefficient as a function of mach number. From fig.5b it can be deduced that for supersonic flow, as the M_∞ increases C_p decreases linearly till $M_\infty=9$. The largest gradient of 17.5% is in the region of $M=5$. For higher Mach numbers the pressure coefficient does not change more than 0.5%. Hence again, Oswatitsch's Mach number independence principle is impressively confirmed at $M_\infty=10$. The results of the theoretical calculation for the pressure distributions about wedges are relatively independent of the Mach number and Reynolds number in the range tested. It can be observed from fig.5b, that Newtonian theory is preferable for predicting the pressure on axisymmetric slender bodies.

3. EVALUATION OF THE OBLIQUE SHOCK WAVE ON A WEDGE

The mean molecular collision time in the gas is much greater than the transit time of the gas passing through the shock wave, and the vector velocity of each molecule differs but negligibly from the free stream velocity. From this, we may conclude that the independence principle applies also to the structures of the shock wave, Ref[1]. Fig.7 shows the variation of shock shapes with Mach number at inviscid flow. The independence principle appears at a relatively higher Mach number for slender bodies in comparison with blunt ones since the shock angle is very high. This analogy can be visualized using Fig.6. Where the Oswatitsch principle is approached at $M_\infty=7$ for the wedge. Numerical and theoretical results show that the shock shapes vary with little difference at higher

Mach number. From the figure, it can be noted that there is a sharp decline in " β " as the Mach number increases to 5. Correspondingly, Conditions immediately behind the shock may be considered to serve as boundary conditions for the flow field. Thus, a flow solution obtained for one sufficiently large value of M_∞ will serve for another large value of M_∞ if P_∞ and velocity are the same. With the assumption of the uniqueness of this type of flow solution, the independence principle follows immediately.

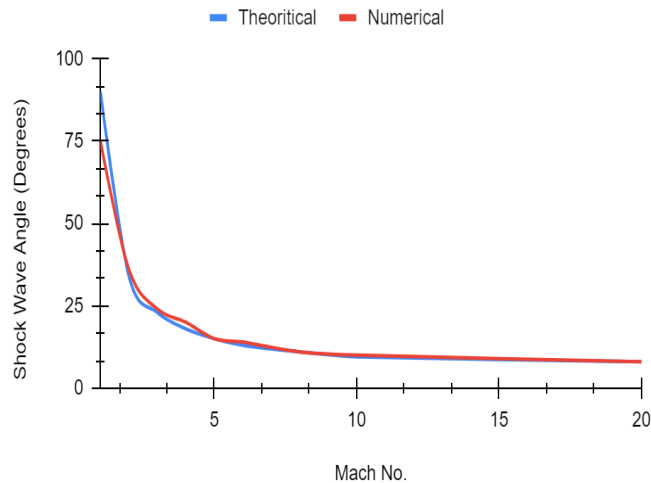


Figure 6-Variation of shock wave angle(β) with Mach number(M_∞)

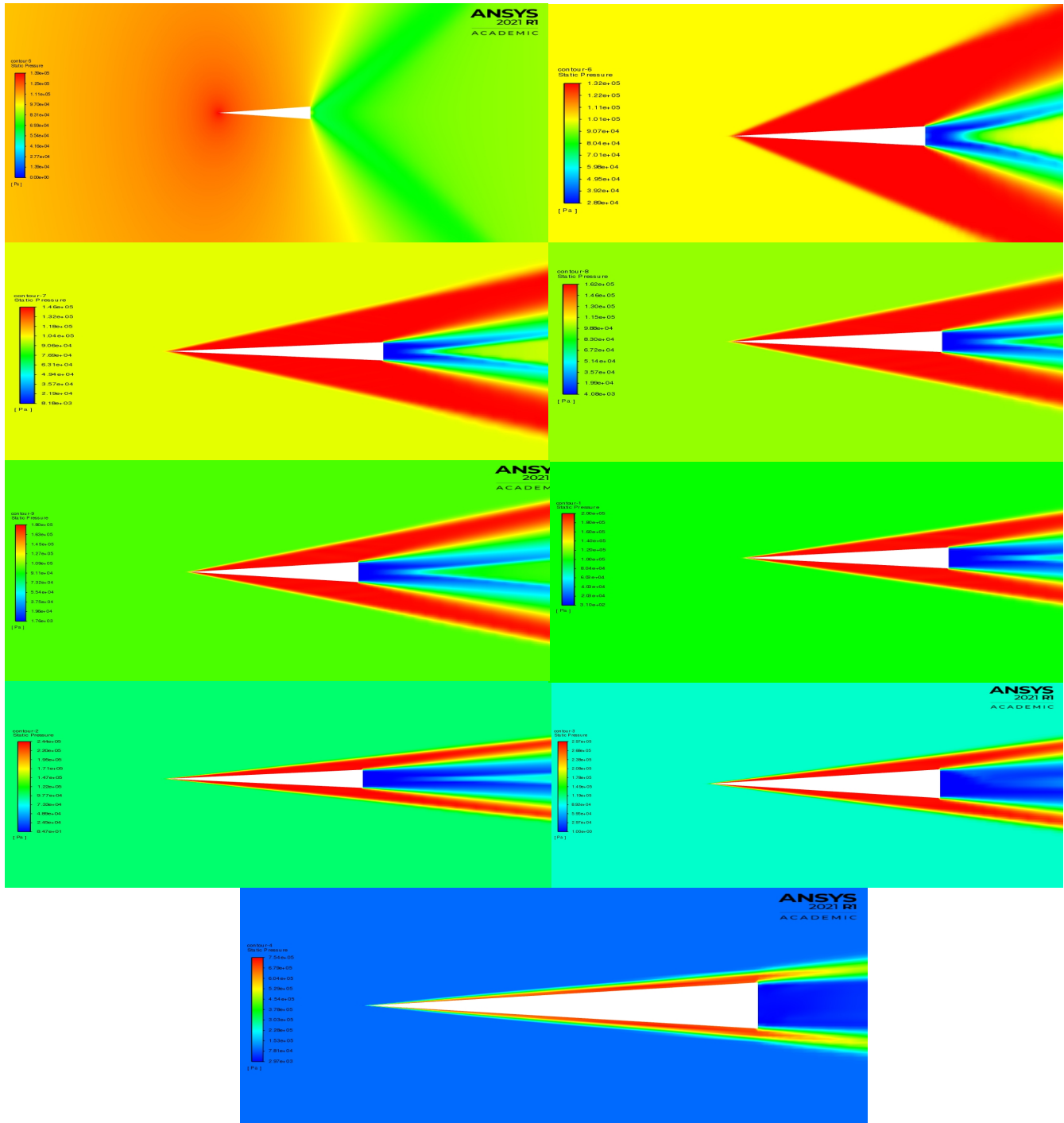


Figure 7-Static pressure contours of mach numbers 2,3,4,5,6,8,10, and 20

CONCLUSION

The applicability of Oswatitsch's independence principle has been seen in R-V type flight vehicles and CAV type flight vehicles. We consider here especially the case of two-dimensional slender bodies. Explicit relations are defined by Oswatitsch, which connect the

shock properties to the body shape, and are available only for the two-dimensional inviscid ramp flow. In a large Mach number range pressure coefficient, drag coefficient, and shock wave shapes vary only weakly across the oblique shocks.

➤ For C_p , the numerical and theoretical results show that the pressure distribution about the 2D wedge is relatively independent of Mach number in the range $2 < M_\infty < 20$, accordingly differ insignificantly from Newton's theory.

➤ For C_D , the results indicate that independence exists for inviscid flow.

➤ Investigations on shock wave angle have indicated the actual validity of Oswatitsch's Mach number independence principle. On the flip side, the viscosity will change the value of wave drag coefficient, pressure coefficient, and influence the shock wave shape at high Mach numbers. Nevertheless, they do not fully prove the validity of the principle in the case of viscous flow and at moderately low Reynolds numbers on slender bodies, the effects of the displacement thickness of the boundary layer may be large enough to invalidate the independence principle.

ACKNOWLEDGMENT

I would like to express my gratitude to Dr. Amallesh Barai, who offered valuable data and statistics which I used in my thesis. I deeply thank my mother, Yashoda for her unconditional trust, timely encouragement, and endless patience. It was her love that raised me again when I got weary.

REFERENCES

1. K. Oswatitsch, Similarity laws for hypersonic flow, Tech. Note No. 16, Institutionen for Flygteknik, Kungl. Tekniska Hogskolan, Stockholm, 1950
2. A. C. Charters, R. N. Thomas, (1945), The aerodynamic performance of small spheres from subsonic to high supersonic velocities, J. Aero. Sci 12, 468-476
3. J. D. Anderson, Modern compressible flow with historical perspective, second edition, McGraw-Hill, New York, 1990
4. D. Kliche, Ch. Mundt and E.H. Hirschel, The hypersonic Mach number independence principle in the case of viscous flow, Shock Waves (2011) 21:307-314
5. A. J. Hodges, (1961), The drag coefficient of very high-velocity spheres. J. Aero. Sci. 24, 755-758
6. K. Oswatitsch, Spezialgebiete der gasdynamik. Schallnahe, Hyperschall, Tragflächen, Wellenausbreitung, pp. 163-1567. Springer, Berlin (1977)
7. W. D. Hayes, R. F. Probstein, Hypersonic flow theory. In: inviscid flows, vol. I. Academic Press, New York (1966).
8. Hayes, W.D.: On hypersonic similitude. Quart. Appl. Math. 5, 179f (1946)
9. Hirschel, E.H.: Basics of Aerothermodynamics, 2nd edn. Springer, Berlin/Heidelberg (2015)
10. Tsien, H.S.: Similarity laws of hypersonic flows. J. Math. Phys. 25, 247f (1946)
11. Ackeret, J.: Habilitationsschrift, ETH Zürich (1928)
12. Anderson, J.D. (1989) Hypersonic and High-Temperature Gas Dynamics. American Institute of Aeronautics and Astronautics, Stanford University, Stanford.
13. Oswatitsch, K. (1951) Ähnlichkeitsgesetze für Hyperschallströmungen. Zeitschrift für Angewandte Mathematik und Physik (ZAMP). (2), 249-264, July 1951.
14. E. SANGER, "Gleitkörper für sehr hohe Fluggeschwindigkeiten," German Patent 411/42, Berlin (1939).
15. Claus Weiland, The aerodynamics of real space vehicles in the light of supersonic and hypersonic approximate theories, CEAS (2019)
16. Volkmar Lorenz, Christian Mundt, A Method for the Solution of the 2D-Oswatitsch Equations, 844-856, April (2016)